




The characteristics of the lobular arrangement indicate the dynamic role played by the infrapatellar fat pad in knee kinematics

Veronica Macchi,^{1,2}  Edgardo Enrico Edoardo Picardi,¹ Chiara Giulia Fontanella,^{2,3} Andrea Porzionato,^{1,2} Carla Stecco,^{1,2}  Cinzia Tortorella,¹ Marta Favero,⁴ Arturo Natali^{2,5} and Raffaele De Caro^{1,2} 

¹Institute of Human Anatomy, Department of Neurosciences, University of Padova, Padova, Italy

²Centre for Mechanics of Biological Materials, University of Padova, Padova, Italy

³Department of Biomedical Sciences, University of Padova, Padova, Italy

⁴Rheumatology Unit, Department of Medicine-DIMED, University Hospital of Padova, Padova, Italy

⁵Department of Industrial Engineering, University of Padova, Padova, Italy

Abstract

The infrapatellar fat pad (IFP) is an intracapsular but extrasynovial structure, located between the patellar tendon, the femoral condyles and the tibial plateau. It consists of white adipose tissue, organised in lobules defined by thin connective septa. The aim of this study is the morphometric and ultrasonographic analysis of IFP in subjects without knee pathology during flexion-extension movements. The morphometric study was conducted on 20 cadavers (15M, 5F, mean age 80.2 years). Ultrasound was performed on 24 volunteers with no history of knee diseases (5M, 19F, mean age: 45 years). The characteristics of the adipose lobules near the patellar tendon and in the deep portion of the IFP were evaluated. Numerical models were provided, according to the size of the lobules. At histological examination, the adipose lobules located near the patellar tendon were larger (mean area $12.2 \text{ mm}^2 \pm 5.3$) than those at a deeper level (mean area $1.34 \text{ mm}^2 \pm 0.7$, $P < 0.001$) and the thickness of the septa of the deepest adipose lobules (mean value $0.35 \text{ mm} \pm 0.32$) was greater than that of the superficial one (mean value $0.29 \text{ mm} \pm 0.25$, $P < 0.001$). At ultrasound, the IFP was seen to be composed of very large lobules in the superficial part (mean area $0.29 \text{ cm}^2 \pm 0.17$ in extension), with a significant reduction in flexion (mean area $0.12 \text{ cm}^2 \pm 0.07$, $P < 0.01$). The deep lobules were smaller (mean area $0.11 \text{ cm}^2 \pm 0.08$ in extension) and did not change their values (mean area $0.19 \text{ cm}^2 \pm 0.52$ in flexion, $P > 0.05$). In the sagittal plane, the reduction of thickness of the superficial layer (with large adipose lobules) during flexion was 20.6%, whereas that of the deep layer (with small adipose lobules) was 1.3%. Numerical simulation of vertical loads, corresponding to flexion of the knee, showed that stress mainly developed within the interlobular septa and opposed bulging of the lobules. The characteristics of the lobular arrangement of the IFP (large lobules with superficial septa in the superficial part and small lobules with thick septa in the deep one), significant changes in the areas and perimeters of the superficial lobules, and the reduced thickness of the superficial layer during flexion all indicate the dynamic role played by the IFP in knee kinematics.

Key words: infrapatellar fat pad; knee; microscopic anatomy; radiological anatomy; ultrasound.

Introduction

The infrapatellar fat pad (IFP; Hoffa, 1904) is an intracapsular but extrasynovial structure, located between the patellar

tendon, the femoral condyles and the tibial plateau (Benninger, 2016). The function of the IFP is still debated and is hypothesised to play a role in the biomechanics of the knee joint (Platzer, 1996; Fontanella et al. 2017). According to the location of the IFP in close contact with the synovial membrane (Geraghty & Spear, 2017) and the metabolic properties of adipose tissue as potential source of adipokines and cytokines (Ioan-Facsinay & Kloppenburg, 2013), the IFP and the synovial membrane are considered a single morpho-functional unit involved in knee osteoarthritis (OA; Favero et al. 2017; Macchi et al. 2018). The

Correspondence

Raffaele De Caro, Department of Neurosciences, Institute of Human Anatomy, University of Padova, Via A. Gabelli 65, 35127 Padova, Italy. T: + 39 049 8272327; F: + 39 049 8272319; E: rdecaro@unipd.it

Accepted for publication 6 March 2019

Article published online 4 April 2019

microscopic characteristics of the IFP show white adipose tissue (fibro-adipose, lobular type), organised in lobules with a mean diameter of $1.15 \text{ mm} \pm 0.11$, defined by thin connective septa (0.22 mm ; Macchi et al. 2016).

Magnetic resonance (MR) is a valuable tool routinely used to assess the IFP (Fontanella et al. 2018) and its disease (Yun et al. 2017). Ultrasound (US) has been reported as an alternative imaging technique for the IFP and shows a characteristic two-layered echo-structure: the superficial adipose tissue is hypochoic with respect to the nearby patellar tendon and contains septae, whereas the deeper layer is homogeneously hypochoic (Vera-Pérez et al. 2017). US enables dynamic and comparative assessment in real time (Naredo, 2015) and some US parameters show significant differences in cases of IFP impingement (Mikkilineni et al. 2018). More detailed knowledge of the dynamic (flexo-extension movements) US characteristics of the IFP in asymptomatic subjects with respect to histological data may be very useful, allowing better understanding of pathological findings.

From the mechanical viewpoint, numerical meso-models are based on several mechanical and geometric properties of each type of adipose tissue: in particular, lobule size and septa thickness can be examined. This approach has been reported to provide IFP cushioning in the knee, with consequent development of adequate mechanical functionality (Fontanella et al. 2017).

Thus, the aims of the present study in subjects without knee pathology were: (1) to analyse the microscopic organisation of the IFP in its superficial part (i.e. near the patellar tendon) and its deep part by morphometrical study, (2) to study the morphological US features of the IFP during flexo-extension movements and (3) to analyse the correlation between histo-morphological configuration and mechanical properties according to a computational approach, to evaluate the mechanical response of the tissues in question.

Materials and methods

The first part of the study was conducted with the approval of the scientific coordinator of the Donation Program (Institute of Human Anatomy, University of Padova) on cadavers: the IFP was sampled for histo-topographical and morphometrical evaluation and numerical analysis. According to the results of these analyses, in the second part of the study the appearance of US in the IFP was evaluated in volunteers, who provided written informed consent. Participants in the study included undergraduate and post-graduate students of the School of Medicine of the University of Padova and also others working at the Institute of Anatomy (technicians, administrative staff, teachers, etc.).

Histo-topographical study

The histo-topographical study was conducted on specimens of IFP sampled from 20 bodies or body parts (15M, 5F; mean age 80.2 years; Macchi et al. 2011) of the Body Donation Programme of

the University of Padova. The inclusion criterion was the absence of history of osteoarthritis. Sections $10 \mu\text{m}$ thick were obtained from paraffin-embedded samples of full-thickness longitudinal samples of the IFP, including subcutaneous tissue and the patellar tendon, and were stained with haematoxylin and eosin (HE; Macchi et al. 2016). These sections were recorded with a high-resolution digital camera (DC 200, Leica Microsystems) and the septa were initially manually identified. The images were then converted to 8-bit binary images for processing with PROGRAMMING LANGUAGE SOFTWARE (Matlab R2012b, MathWorks Inc., Natick, MA, USA). The superficial and deep adipose lobules were automatically approximated to ellipses and their areas and major and minor axes were calculated (Macchi et al. 2016). These data were then adopted for subsequent evaluation of the mechanical response of tissues by computational analysis.

Numerical analysis

The mechanical response of the IFP was strongly influenced by its structural conformation, e.g. the dimensions of adipose lobules (Natali et al. 2012a,b). Numerical analyses were performed to study the mechanical behaviour of the IFP, with the procedure adopted and described in Fontanella et al. (2017). In the previous work, the IFP was considered to show a homogeneous, constant distribution of adipose lobules. In this study, two numerical models were provided to take into account variations in chamber dimensions, such as macro- and micro-chambers. Hyperelastic isotropic and anisotropic constitutive models (Carniel et al. 2014; Fontanella et al. 2017) were developed to interpret the mechanical behaviour of adipose lobules and connective septa, respectively. The response of the tissues was evaluated under unconfined compression loads with ABAQUS/CAE 6.14 finite-element software (Abaqus Documentation 2014, Dassault Systèmes Simulia Corp., Providence, RI, USA), to enhance the correlation between the structural conformation and mechanical properties of the tissues in question (Fontanella et al. 2017).

Anatomo-radiological study

In this study, 24 healthy subjects (5M, 19F, mean age: 45 years; range 21–70) were analysed, and 48 knees were evaluated by US. The subjects were volunteers and the inclusion criteria were the absence of history of knee diseases and a negative clinical knee joint examination and Hoffa's test, performed by an orthopaedic surgeon (C.S.). Examinations were performed by an ultrasonographer with 10 years of experience (V.M.), using high-resolution grey-scale ultrasound (Sonosite, Bothell, WA, USA). A multifrequency (8–13 MHz) linear probe was used and the scanning protocol included multiple scans to evaluate the IFP. Subjects were examined in the supine position, first with the knee extended and then flexed at 90° .

Measurements were taken in midline sagittal sections. The patellar tendon was scanned vertically and the following parameters were recorded:

- area and perimeter of one (superficial) US adipose lobule closest to the patellar tendon in extension and flexion;
- area and perimeter of one of the deepest recognisable US adipose lobules in extension and flexion.

A comparative examination of both knees was performed. In fact, according to the results of the histo-topographical study and

in order to visualise the same lobule in both flexion and extension, the parameters of one adipose lobule were examined, in view of the need for precise topographical criteria for location.

The IFP was also divided into two layers, according to the results of the histo-topographical study, and showed the presence of large adipose lobules (macro-chambers) in the superficial part of the IFP and small adipose lobules (micro-chambers) in its deepest part (Hsu et al. 2007). A line was traced parallel to the patellar tendon, and half the distance between the hypo-echogenicity of the femoral condyle and the tibial plate was detected; a line perpendicular to the former was then traced from the patellar tendon to the deepest part of the IFP (Fig. 1). The thicknesses (th) of all the IFP, of the macro-chamber (th_{mac}) and of the micro-chamber (th_{mic}) layers were measured. The thickness of these two layers was also measured in extension (th ; th_{mac} ; th_{mic}) and flexion (th' ; th'_{mac} ; th'_{mic}). Subsequently, variations in thickness of both macro- and micro-chambers were calculated as $\Delta X_{mac} = th_{mac} - th'_{mac}$ and $\Delta X_{mic} = th_{mic} - th'_{mic}$, respectively. Any deformation in both chambers was defined as follows:

$$\varepsilon_{mac} = \frac{\Delta X_{mac}}{th_{mac}}; \varepsilon_{mic} = \frac{\Delta X_{mic}}{th_{mic}}$$

The proportion of maximum macro-chamber tissue deformation to the maximum overall deformation was defined as $\frac{\Delta X_{mac}}{\Delta X_{mac} + \Delta X_{mic}}$ and the proportion of maximum micro-chamber tissue deformation to the maximum overall deformation was defined as $\frac{\Delta X_{mic}}{\Delta X_{mac} + \Delta X_{mic}}$. The proportion of maximum deformation revealed the contribution of deformation of each layer during the examination.

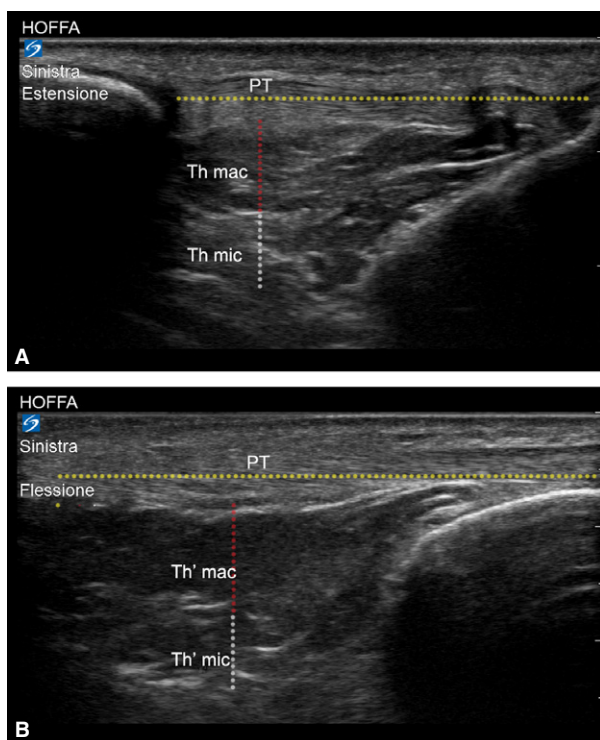


Fig. 1 US analysis of deformation variations of macro- and micro-chambers of infrapatellar fat pad. Thickness (th) of macro- (th_{mac}) and micro-chamber (th_{mic}) layers in flexion (A). Thickness (th) of macro- (th_{mac}) and micro-chamber (th_{mic}) layers in extension (B).

Statistical analysis

Results are reported as mean (\pm SD) values and ranges. Statistical analyses were performed with Student's *t*-test, with $P < 0.05$ as significant and linear correlations (GRAPHPAD Software Inc., San Diego, CA, USA).

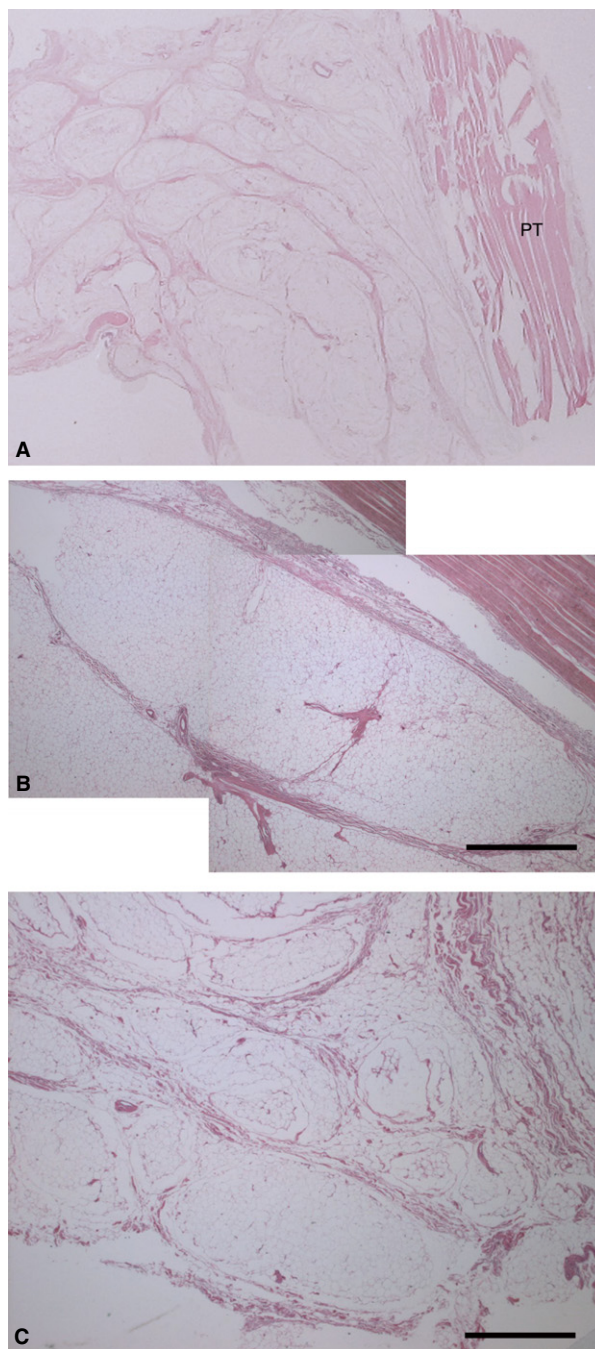


Fig. 2 Macro-section of infrapatellar fat pad (A), consisting of white adipose tissue organised in lobules, larger near patellar tendon (B) and smaller at deep level (C). Thickness of interlobular septa of IFP was homogeneous at both levels. Haematoxylin-eosin stain. Scale bar: 1 mm.

Table 1 Data of morphometric study (mean values \pm SD).

Morphometry	Superficial	Deep	<i>P</i> -value
Area (mm ²)	12.2 \pm 5.3	1.34 \pm 0.75	< 0.01
Thickness of septa (mm)	0.29 \pm 0.25	0.35 \pm 0.32	< 0.01

Results

Histo-topographical study

The histo-topographical study showed that the IFP consisted of white adipose tissue organised in clearly defined lobules by connective septa of various sizes, and round or oval in shape, from those closest to the patellar tendon to the deepest ones. In particular, the average area of the adipose lobules closest to the patellar tendon (i.e. superficial) was 12.2 mm² \pm 5.3, significantly greater than that of the deepest lobules, with 1.34 mm² \pm 0.7 (*P* < 0.01; Fig. 2). The major and minor axes of the adipose lobules closest to the patellar tendon were greater than those of the deepest ones (*P* < 0.01; Table 1). Interestingly, the mean thickness of the septa of the deepest lobules was 0.35 mm \pm 0.32, greater than that of the superficial ones (0.29 mm \pm 0.25).

Ultrasound study

At US, the IFP appeared to be composed of hypo-echoic structures, with round or oval shapes, ascribable to US lobules; oblique hyper-echoic lines were identified at the boundaries of these structures. This arrangement corresponded to the microscopic appearance of the IFP, organised as it was in US lobules defined by interlobular septa. The shape and area of the lobules appeared to change

during dynamic examination. The mean sagittal area of the deepest US adipose lobule was 0.11 cm² in extension and 0.19 cm² in flexion, and the perimeter was 1.36 cm in extension and 1.2 cm in flexion. The area of the US adipose lobule closest to the patellar tendon was 0.29 cm² in extension and 0.12 cm² in flexion (*P* < 0.01), whereas the perimeter was 2.67 cm in extension and 1.56 cm in flexion (*P* < 0.01; Fig. 3). There were no statistically significant differences in area or perimeter between males or females or between right or left sides, or any correlations with age (Table 2).

The mean thickness of the whole IFP was 3.63 \pm 0.40 cm, and that of the macro- and micro-chambers was 2.14 \pm 0.25, and 1.5 \pm 0.14 cm of the latter in extension. The variation in thickness of the macro-chambers, Δth_{macr} was 0.44 \pm 0.10 cm, and that of the micro-chambers Δth_{mic} was 0.02 \pm 0.06 cm (*P* < 0.01). The deformation of the macro-chambers was 20.6% and that of the micro-chambers 1.3%. The proportion of thickness variations of the macro-chamber to the maximum overall deformation was 95%, and that of the micro-chambers to the maximum overall deformation was 5% (Table 3), showing that the macro-chambers made a greater contribution to the overall IFP deformation.

Numerical analysis

The actual functionality of micro- and macro-chambers was revealed by numerical simulation of compressive load. Under vertical loading, i.e. flexion, the IFP structures produced differing mechanical responses (Fig. 4). Numerical results were reported at the same load (15 N), showing greater deformation in macro- than in micro-chambers. Their different conformations in terms of adipose lobules and interlobular septa contributed differently to the overall

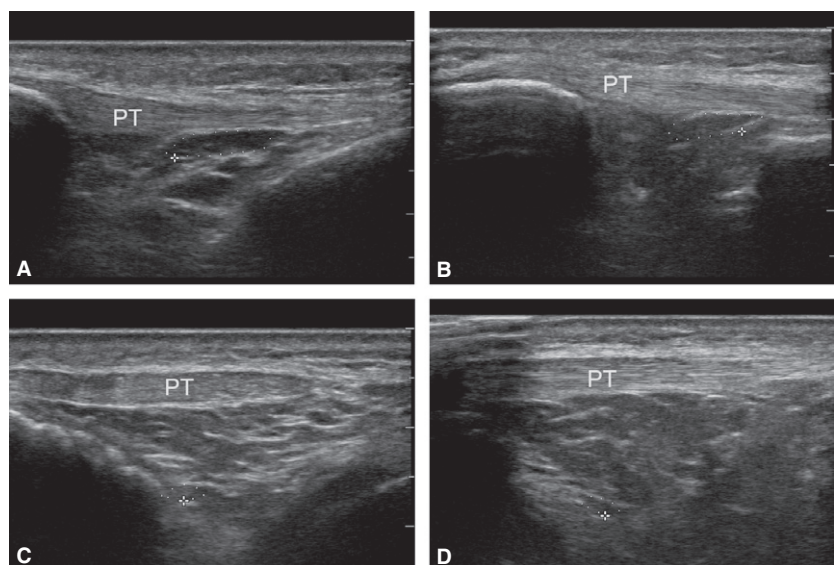


Fig. 3 US examination of infrapatellar fat pad. Analysis of area and perimeter of adipose chamber closest to patellar tendon (PT) in extension (A) and flexion (B). Analysis of area and perimeter of deepest identifiable adipose chamber in extension (C) and flexion (D).

Table 2 Data of ultrasound study.

Ultrasound	Extension	Flexion	P-value
Superficial area (cm ²)	0.29 ± 0.17	0.12 ± 0.07	< 0.01
Superficial perimeter (cm)	2.67 ± 0.76	1.56 ± 0.44	< 0.01
Deep area (cm ²)	0.11 ± 0.08	0.19 ± 0.52	> 0.05
Deep perimeter (cm)	1.36 ± 0.39	1.20 ± 0.53	> 0.05

Ultrasound	Right	Left	P-value
Extension superficial area (cm ²)	0.31 ± 0.15	0.27 ± 0.19	> 0.05
Flexion superficial area (cm ²)	0.11 ± 0.08	0.12 ± 0.07	> 0.05
Extension superficial perimeter (cm)	2.79 ± 0.74	2.54 ± 0.79	> 0.05
Flexion superficial perimeter (cm)	1.52 ± 0.46	1.60 ± 0.43	> 0.05
Extension deep area (cm ²)	0.11 ± 0.06	0.12 ± 0.11	> 0.05
Flexion deep area (cm ²)	0.09 ± 0.07	0.29 ± 0.75	> 0.05
Extension deep perimeter (cm)	1.48 ± 0.32	1.23 ± 0.43	> 0.05
Flexion deep perimeter (cm)	1.16 ± 0.40	1.24 ± 0.65	> 0.05

Ultrasound parameters	Female	Male	P value
Extension superficial area (cm ²)	0.29 ± 0.19	0.28 ± 0.09	> 0.05
Flexion superficial area (cm ²)	0.11 ± 0.06	0.14 ± 0.09	> 0.05
Extension superficial perimeter (cm)	2.62 ± 0.85	2.81 ± 0.45	> 0.05
Flexion superficial perimeter (cm)	1.48 ± 0.33	1.77 ± 0.64	> 0.05
Extension deep area (cm ²)	0.11 ± 0.09	0.12 ± 0.08	> 0.05
Flexion deep area (cm ²)	0.23 ± 0.60	0.08 ± 0.04	> 0.05
Extension deep perimeter (cm)	1.32 ± 0.38	1.47 ± 0.42	> 0.05
Flexion deep perimeter (cm)	1.24 ± 0.59	1.08 ± 0.27	> 0.05

Ultrasound parameters	< 45 years old	> 45 years old	P-value
Extension superficial area (cm ²)	0.33 ± 0.18	0.25 ± 0.16	> 0.05
Flexion superficial area (cm ²)	0.14 ± 0.09	0.10 ± 0.05	> 0.05
Extension superficial perimeter (cm)	2.9 ± 0.65	2.46 ± 0.81	> 0.05
Flexion superficial perimeter (cm)	1.71 ± 0.54	1.42 ± 0.27	> 0.05
Extension deep area (cm ²)	0.14 ± 0.10	0.09 ± 0.05	> 0.05
Flexion deep area (cm ²)	0.32 ± 0.75	0.06 ± 0.04	> 0.05
Extension deep perimeter (cm)	1.41 ± 0.45	1.32 ± 0.33	> 0.05
Flexion deep perimeter (cm)	1.35 ± 0.71	1.06 ± 0.22	> 0.05

mechanical properties of the tissues. Tensile stress mainly developed within interlobular septa and opposite to bulging of adipose lobules. Micro-chambers had a larger

Table 3 Mechanical properties of micro-chamber and macro-chamber layers in infrapatellar fat pad.

	Macro-chamber	Micro-chamber	P-value
Thickness in extension, th, mm*	2.14 (0.25)	1.52 (0.14)	< 0.01
Thickness in flexion, th', mm*	1.70 (0.2)	1.50 (0.1)	< 0.01
Thickness variation, Δth, mm*	0.44 (0.1)	0.02 (0.1)	< 0.01
Deformation, ε	20.6%	1.3%	
Proportion of thickness variation O Overall thickness variation	95%	5%	< 0.01

Values are means (SD).

*Student's *t*-test for differences among variables.

number of stressed interlobular septa, showing greater stiffness than the interlobular septa of the macro-chambers. Instead, adipose lobules were less stiff than connective septa. Consequently, the adipose lobules of the micro-chambers deformed less than those of the macro-chambers. Because of the different dimensions of the former, the latter revealed greater strain in adipose lobules than in micro-chambers (Fig. 4).

Discussion

The ultrasound of IFP has recently been reported as an alternative imaging technique, patient-friendly, safe, and also non-invasive and less expensive than MR, enabling dynamic and comparative assessment in real time (Bayar et al. 2008; Naredo, 2015). This study analyses the microscopic and ultrasound characteristics of the IFP in healthy subjects, for better understanding of changes in US parameters in pathological conditions. As *in vivo* dynamic data of changes in IFP during movements are rarely reported, thanks to the widespread use of this radiological method, this study may represent a first step in the correlation between microscopic findings and the ultrasound arrangement of the IFP analysed during flexo-extension movements in the normal population.

The IFP is organised into two clearly defined tissue layers: one superficial, generally resembling the adjacent extra-articular subcutaneous fat, with greater elasticity, and a deeper homogeneously hypo-echoic layer, without interlobular septa (Vera-Pérez et al. 2017). Our histo-topographical analysis does in fact show that the IFP consists of white adipose tissue: the lobules closer to the patellar tendon are larger than the deeper ones ($P < 0.001$) and the interlobular septa are thicker in the deeper levels. The variation in size of lobules inside the IFP may be due to the varying arrangements of the interlobular septa, which

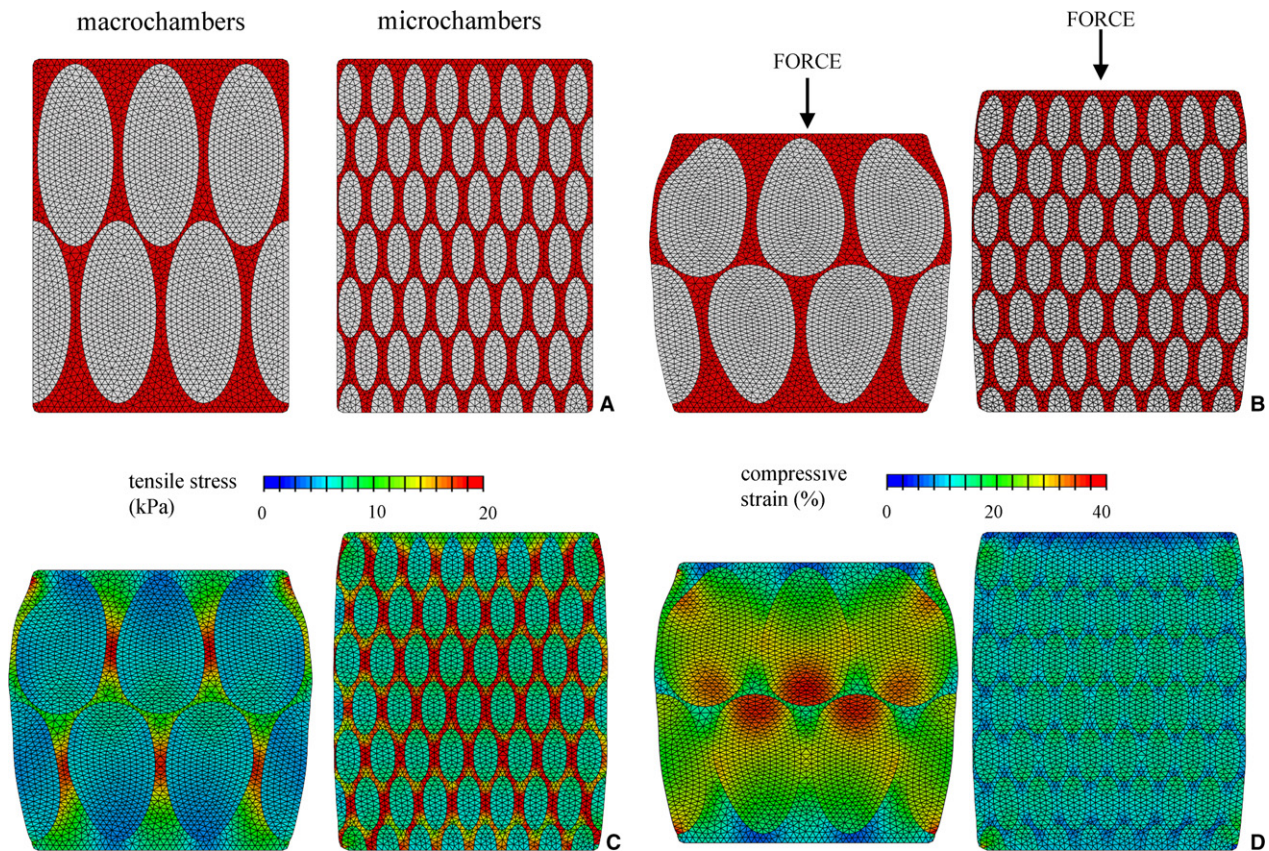


Fig. 4 Numerical models of macro- and micro-chambers, composed of interlobular septa and adipose lobules: initial conformation (A) and deformed configuration under unconfined compressive loading (B). Results from numerical analysis of compression loading. Distribution of tensile stress (C) and compressive strain (D) fields for macro- and micro-chambers at same load level.

are the result of force vectors during knee movements. These structural characteristics of the IFP explain the three-dimensional mesh connecting the epitenon of the patellar tendon to the synovial membrane. This mesh acts as a mechanoreceptor working in the proprioceptive regulation of knee kinematics, due to the extensive distribution of nerves in the IFP and its peculiar configuration (Macchi et al. 2016).

This type of organisation with lobules of various sizes in the superficial and deeper parts may reflect the mechanical property of the IFP, affecting the overall mechanical response. To analyse the relationship between histo-morphological configuration and mechanical properties, finite element micro-models were developed, based on the mechanical properties and geometric configuration of the specific tissue subcomponents. The reliability of the procedure has previously been reported in works analysing the mechanical behaviour of foot adipose tissues (Gurumurthy et al. 2017; Fontanella et al. 2018). In other fat pads, such as the calcaneal fat pad, differences in lobule sizes have been reported (Natali et al. 2010, 2012a,b): small adipose chambers are found close to the dermis, and their dimensions progressively increase towards the calcaneum.

Vertically oriented chambers are located in the central portion of the calcaneal fat pad, whereas chambers are smaller and more transversally oriented in the lateral and posterior regions (Jahss et al. 1992; Natali et al. 2012b). The configuration found in IFP determines the actual mechanical response of the tissues in various loading configurations, stressing the fact that the morphological configuration influences the biomechanical response. Comparison of results from numerical studies on the macro- and micro-chambers confirms the differing responses according to the characteristics of geometric conformations. Numerical results allow us to identify the different stress and strain fields within the tissues, for better understanding of the mechanical role of the IFP in the overall functionality of the knee joint.

Functional changes in the IFP have been explored by imaging. In particular, IFP impingement has been hypothesised to be a dynamic phenomenon. High-resolution US can reveal the various sites of IFP impingement in both knee flexion and extension: in fact, the supra-lateral portion of the IFP has been reported to adopt a relaxed, freely expansive and relatively fluid state in flexion (Mace et al. 2016). Our study is the first to document that the thickness of the

superficial part of the IFP, i.e. the macro-chambers, changes during knee movement. In addition, the characteristics of the superficial US adipose lobules have been found to change in both area and perimeter during flexion. These data match the changes in the antero-posterior distance of the largest US fat lobule measured at 0° and 90° by US, described by Mikkilineni et al. (2018) as a value which determines the percentual compressibility of the lobule itself. Changes in superficial US adipose lobules may also reflect differences in the radius of the curvature between the superficial and deep locations of the IFP in the flexed knee.

We have also demonstrated that, during flexion, the thickness of the IFP is reduced, due to the greater contribution of the superficial (i.e. micro-chamber) adipose layer, by up to 95% of deformation. However, a change in the configuration of the IFP has also been demonstrated by US, with a reduction in the size of the acoustic window with increasing flexion and loss of the discernible two-layered pattern (Vera-Pérez et al. 2017), accounting for the changed morphology of the adipose lobules.

Our study had the following limitations: The analysed population was represented by a small number of volunteers, mostly women. This is because the subjects were undergraduate and post-graduate students of the School of Medicine of the University of Padova, with a prevalence of female subjects. However, no statistically significant differences were found with reference to gender (Macchi et al. 2016). The histo-topographical study was conducted in another group of subjects, not those of the US study. However, the general configuration of adipose lobules in the superficial and deep layers was confirmed in all specimens and, due to the intrinsic characteristics of adipose tissue, postmortem changes due to differences in vascular supply, hydration or temperature (Klauser et al. 2013) may have affected the US examination of cadaver. No pathological subjects were analysed: in pathological IFP, it will be very interesting to evaluate whether adipose lobules can change their configuration, as IFP in knee osteoarthritis shows the increased thickness of the interlobular septa with respect to that of controls, although no differences were detected in the mean diameter of osteoarthritic adipose lobules in the IFP (Favero et al. 2017).

Conclusions

The present study is the first description of changes in the adipose configuration of the IFP during flexo-extension movement of the knee, studied according to a non-invasive method. The histo-topographical arrangement of the adipose lobules shows a peculiar configuration, with large lobules close to the patellar tendon and small ones at the deep level. The use of numerical models based on the present data may contribute to our understanding of the biomechanical role of the IFP in knee kinematics.

Acknowledgements

The authors are grateful to Drs Alessandro Frigo, Anna Rambaldo, Gloria Sarasin and Maria Martina Sfriso for their skilful technical assistance.

Funding

This work was funded by the University of Padova (CDPA 155521).

Conflict of interest

The authors declare that this research was conducted without any kind of funding which might be construed as a potential conflict of interest.

Author contributions

Conception or design of text: V.M., C.G.F., A.N., R.D.C. Acquisition of data, data analysis and interpretation: V.M., E.E.E.P., A.P., C.G.F., C.S., R.D.C. Drafting of manuscript: V.M., E.E.E.P., C.G.F., C.T., A.N., R.D.C. Critical revision and final approval of manuscript: all authors.

References

- Bayar A, Turhan E, Ozer T, et al. (2008) The fate of patellar tendon and infrapatellar fat pad after arthroscopy via central portal. *Knee Surg Sports Traumatol Arthrosc* **16**, 1114–1120.
- Benninger B (2016) Knee. In: *Gray's Anatomy*, 40th edn. (ed. Standring S), p. 1395. London: Elsevier.
- Carniel EL, Gramigna V, Fontanella CG, et al. (2014) Constitutive formulations for the mechanical investigation of colonic tissues. *J Biomed Mater Res A* **102**, 1243–1254.
- Favero M, El-Hadi H, Belluzzi E, et al. (2017) Infrapatellar fat pad features in osteoarthritis: a histopathological and molecular study. *Rheumatology (Oxford)* **56**, 1784–1793.
- Fontanella CG, Carniel EL, Frigo A, et al. (2017) Investigation of biomechanical response of Hoffa's fat pad and comparative characterization. *J Mech Behav Biomed Mater* **67**, 1–9.
- Fontanella CG, Belluzzi E, Rossato M, et al. (2018) Quantitative MRI analysis of infrapatellar and suprapatellar fat pads in normal controls, moderate and end-stage osteoarthritis. *Ann Anat* **221**, 108–114.
- Geraghty RM, Spear M (2017) Evidence for plical support of the patella. *J Anat* **231**, 698–707.
- Gurumurthy B, Bierdeman P, Janorkar AV (2017) Spheroid model for osteogenic evaluation of human adipose derived stem cells. *J Biomed Mater Res A* **105**, 1230–1236.
- Hoffa A (1904) The influence of the adipose tissue with regard to the pathology of the knee joint. *J Am Med Assoc* **3**, 795–796.
- Hsu CC, Tsai WC, Wang CL, et al. (2007) Microchambers and macrochambers in heel pads: are they functionally different? *J Appl Physiol* **102**, 2227–2231.
- Ioan-Facsinay A, Kloppenburg M (2013) An emerging player in knee osteoarthritis: the infrapatellar fat pad. *Arthritis Res Ther* **15**, 225.

- Jahss M, Kummer F, Michelson JD** (1992) Investigation into the fat pads of the sole of the foot: heel pressure studies. *Foot Ankle Int* **13**, 227–232.
- Klauser AS, Miyamoto H, Tamegger M, et al.** (2013) Achilles tendon assessed with sonoelastography: histologic agreement. *Radiology* **267**, 837–842.
- Macchi V, Porzionato A, Stecco C, et al.** (2011) Body parts removed during surgery: a useful training source. *Anat Sci Educ* **4**, 151–156.
- Macchi V, Porzionato A, Sarasin G, et al.** (2016) The infrapatellar adipose body: a histotopographic study. *Cells Tissues Organs* **201**, 220–231.
- Macchi V, Stocco E, Stecco C, et al.** (2018) The infrapatellar fat pad and the synovial membrane: an anatomo-functional unit. *J Anat* **233**, 146–154.
- Mace J, Bhatti W, Anand S** (2016) Infrapatellar fat pad syndrome: a review of anatomy, function, treatment and dynamics. *Acta Orthop Belg* **82**, 94–101.
- Mikkilineni H, Delzell PB, Andrish J, et al.** (2018) Ultrasound evaluation of infrapatellar fat pad impingement: an exploratory prospective study. *Knee* **25**, 279–285.
- Naredo E** (2015) Ultrasound in rheumatology: two decades of rapid development and evolving implementation. *Med Ultrason* **17**, 3–4.
- Natali AN, Fontanella CG, Carniel EL** (2010) Constitutive formulation and analysis of heel pad tissue mechanics. *Med Eng Phys* **32**, 516–522.
- Natali AN, Fontanella CG, Carniel EL** (2012a) Constitutive formulation and numerical analysis of the heel pad region. *Comput Methods Biomech Biomed Engin* **15**, 401–409.
- Natali AN, Fontanella CG, Carniel EL** (2012b) A numerical model for investigating the mechanics of the calcaneal fat pad region. *J Mech Behav Biomed Mater* **5**, 216–223.
- Platzer W** (1996) Anatomy of the knee. In: *Atlas van de Anatomie, vol. 1*, 7th edn. (ed. Platzer W), p. 462. Baarn: Sesam.
- Vera-Pérez E, Sánchez-Bringas G, Ventura-Ríos L, et al.** (2017) Sonographic characterization of Hoffa's fat pad. A pilot study. *Rheumatol Int* **37**, 757–764.
- Yun SJ, Lim Y, Jin W, et al.** (2017) Validity of radiograph-based infrapatellar fat pad opacity grading for assessing knee synovitis: correlation with contrast-enhanced MRI. *AJR Am J Roentgenol* **209**, 1321–1330.